

The Effect of Orbital Eccentricity on Gravitational Wave Background Radiation from Supermassive Black Hole Binaries

Motohiro ENOKI^{1,*} and Masahiro NAGASHIMA^{2,3}

¹*National Astronomical Observatory of Japan, Mitaka 181-8588, Japan*

²*Department of Physics, Kyoto University, Kyoto 606-8502, Japan*

³*Faculty of Education, Nagasaki University, Nagasaki 852-8521, Japan*

A compact binary in an eccentric orbit radiates gravitational waves (GWs) at all integer harmonics of its orbital frequency. In this study, we investigate the effect of orbital eccentricity on the expected gravitational background radiation (GWB) from supermassive black hole (SMBH) binaries in the nuclei of galaxies. For this purpose, we formulate a power spectrum of the GWB from cosmological evolving eccentric binaries. Then, we apply this formulation to the case of the GWB from SMBH binaries. The key to doing this is to correctly estimate the number density of coalescing SMBH binaries. In this study, we use a semi-analytic model of galaxy and SMBH formation. We find that the power spectrum of the GWB from SMBH binaries on eccentric orbits is suppressed for frequencies $f \lesssim 1$ nHz if the initial eccentricity, e_0 , satisfies $e_0 > 0.2$ and the initial semi-major axis is 300 times Schwarzschild radius. Our model predicts that while the overall shape and amplitude of the power spectrum depend strongly on the processes of galaxy formation, the eccentricity of binaries can affect the shape of the power spectrum for lower frequencies, i.e., $f \lesssim 1$ nHz. Pulsar timing measurements, which can detect GW in this frequency range, could constrain the effect of eccentricity on the power spectrum of the GWB from SMBH binaries.

§1. Introduction

An ensemble of gravitational waves (GWs) from a number of inspiraling binaries of compact objects at different redshifts can be observed as stochastic gravitational wave background radiation (GWB). Coalescing supermassive black hole (SMBH) binaries with masses in the range $10^6 - 10^9 M_\odot$ emit GWs, as a result of the merging of their host galaxies. Recent studies^{1),2)} predict that these SMBH binaries produce GWB of frequencies ~ 1 n – 1 μ Hz. In the frequency range 0.1 m – 10 mHz, it is believed that extragalactic close binaries of white dwarfs are dominant sources of GWB.³⁾

Gravitational waves with frequencies in the range 1 n – 100 nHz can be detected by pulsar timing measurements.⁴⁾ Thus we should be able to detect the GWB from SMBH binaries directly. Recently, Jenet et al.⁵⁾ developed a new method for detecting GWB using multiple pulsar timing data. In the case of the Parkes Pulsar Timing Array (PPTA) project,^{6)**)} their results showed that with regular timing observations of 20 pulsars with a timing accuracy of 100 ns, we should be able to directly detect the predicted levels of the GWB from SMBH binaries within five years.⁵⁾

In previous studies^{1),2)} of the GWB from SMBH binaries, it was assumed that all binaries are in circular orbits. However, binary orbits are generally eccentric.

*) E-mail: enoki.motohiro@nao.ac.jp

***) See <http://www.atnf.csiro.au/research/pulsar/array/>

Before entering into the GW emitting regime, the evolution of a SMBH binary is determined by its dynamical interaction with field stars in the center of its host galaxy. Mikkola and Valtonen⁷⁾ constructed approximate expressions relating the energy and angular momentum transfer rates for a heavy binary and the surrounding field of light stars, and they showed that the length of the semi-major axis decreases and the eccentricity increases owing to dynamical friction. Fukushige et al.⁸⁾ investigated the evolution of a SMBH binary in a uniformly distributed background of field stars and found that the dynamical friction on the eccentric binary is most effective at the apocenter, where the orbital velocity is minimum, and thus the eccentricity increases. Iwasawa et al.⁹⁾ performed N -body simulations of the dynamical evolution of triple SMBH (a binary of SMBHs and a single SMBH) systems in galactic nuclei and showed that the eccentricity of the SMBH binary reaches $e > 0.9$ in the GW emission regime. They found that both the Kozai mechanism and the thermalization of eccentricity due to the strong binary-single SMBH interaction drive the increase of the orbital eccentricity. Matsubayashi et al.¹⁰⁾ investigated the orbital evolution of intermediate mass black hole (IMBH)-SMBH systems in galactic centers, using N -body simulations. They found that the eccentricity approaches unity ($e > 0.8$) and the IMBH can cause the SMBH to rapidly coalesce as a result of GW emission. Armitage and Natarajan¹¹⁾ studied the evolution of the SMBH binary eccentricity which is excited by the interaction between a binary and circumbinary gas disk. They estimated a typical eccentricity at one week prior to coalescence to be $e \sim 0.01$. In the case of extreme-mass ratio binaries, higher eccentricities ($e \sim 0.1$) are possible.

An eccentric binary emits GWs at all integer harmonics of the orbital frequency.^{12),13)} Thus, the spectral energy distribution (SED) is different from that of a binary in a circular orbit, even if the masses and semi-major axes of the two binaries are the same. For larger eccentricities, radiation from higher harmonics are greater and thus the peak of the SED shifts toward higher frequency. Moreover, the orbital evolution of a binary due to GW radiation depends strongly on its eccentricity. As a result, the power of GW radiation of an eccentric binary is larger than that of a circular binary, and the timescale of GW radiation of an eccentric binary is shorter than that of a circular binary. Therefore, in order to predict the power spectrum of GWBR from compact binaries, it is necessary to take account of orbital eccentricities of binaries. For the cases of GWBRs from galactic and extragalactic neutron star binaries and black hole MACHO binaries, some studies have taken account of the effect of eccentricity.^{3),15)} However, for the case of the GWBR from SMBH binaries, none of models include the effect of eccentricity.

In this study, we investigate the effect of orbital eccentricity on the expected GWBR from SMBH binaries. First, we formulate the power spectrum of GWBR from cosmological eccentric binaries, taking into account eccentricity evolution. In order to formulate the power spectrum, we adopt a simple relationship between the power spectrum of the GWBR produced by cosmological GW sources, the total time-integrated energy spectrum of individual sources, and the comoving number density of GW sources found by Phinney.¹⁴⁾ Next, we apply this formulation to the case of the GWBR from coalescing SMBH binaries. In order to estimate the number density of SMBH binaries, we use a semi-analytic (SA) model¹⁷⁾ in which SMBH

formation is incorporated into galaxy formation.¹⁶⁾

This paper is organized as follows. In §2 we briefly review the GW emission of a binary in an eccentric orbit. In §3 we formulate the power spectrum of GWBR from cosmological compact binaries in eccentric orbits. In §4 we present the power spectrum of the GWBR from eccentric SMBH binaries. In §5 we present a summary and conclusions.

§2. GWs from a binary in an eccentric orbit

Here we briefly review the situation for GWs emitting from a binary in an eccentric orbit and the evolution of a binary due to GW emission in the weak field, slow motion limit.^{12),13)}

The total power of the GW emission from a Keplerian binary consisting of two point masses M_1 and M_2 , with orbital frequency f_p and orbital eccentricity e is

$$L_{\text{GW}}(M_1, M_2, f_p, e) = L_{\text{GW,circ}}(M_1, M_2, f_p)F(e), \quad (2.1)$$

where

$$\begin{aligned} L_{\text{GW,circ}}(M_1, M_2, f_p) &= \frac{32}{5} \frac{G^{7/3}}{c^5} M_{\text{chirp}}^{10/3} (2\pi f_p)^{10/3} \\ &= 4.7 \times 10^{48} \left(\frac{M_{\text{chirp}}}{10^8 M_\odot} \right)^{10/3} \left(\frac{2f_p}{10^{-7} \text{ Hz}} \right)^{10/3} \text{ erg}, \end{aligned} \quad (2.2)$$

and

$$F(e) \equiv \frac{1 + 73e^2/24 + 37e^4/96}{(1 - e^2)^{7/2}}. \quad (2.3)$$

The quantity $L_{\text{GW,circ}}(M_1, M_2, f_p)$ is the total power from a binary in a circular orbit with masses M_1 and M_2 and orbital frequency f_p . This is equal to the reciprocal of the proper rest-frame period of the binary. In the above expressions, G is the gravitational constant, c is the speed of light, and $M_{\text{chirp}} \equiv [M_1 M_2 (M_1 + M_2)^{-1/3}]^{3/5}$ is the chirp mass of the system. The distribution of the total power of GW emission among the harmonics of the orbital frequency is given by $L_{\text{GW,circ}}(M_1, M_2, f_p)g(n, e)$, with the rest-frame GW frequency $f_r = n f_p$. Here, $g(n, e)$ is the GW frequency distribution function, expressed as

$$\begin{aligned} g(n, e) &\equiv \frac{n^4}{32} \left\{ \left[J_{n-2}(ne) - 2eJ_{n-1}(ne) + \frac{2}{n}J_n(ne) + 2eJ_{n+1}(ne) - J_{n+2}(ne) \right]^2 \right. \\ &\quad \left. + (1 - e^2) [J_{n-2}(ne) - 2eJ_n(ne) + J_{n+2}(ne)]^2 + \frac{4}{3n^2} [J_n(ne)]^2 \right\}, \end{aligned} \quad (2.4)$$

where J_n is the n th-order Bessel function. It can be shown that

$$\sum_{n=1}^{\infty} g(n, e) = F(e). \quad (2.5)$$

For the case of a circular orbit (i.e., $e = 0$), we have $g(2, 0) = 1$ and $g(n, 0) = 0$ for all $n \neq 2$. The SED of gravitational radiation is given by

$$L_{f_r}(e, t_p) = L_{\text{GW,circ}}(f_p) \sum_{n=1}^{\infty} g(n, e) \delta(f_r - n f_p). \quad (2.6)$$

Here, t_p is the time at which the orbital frequency is f_p , and $\delta(x)$ is Dirac's delta function.

The timescale of GW emission by a binary with orbital frequency f_p measured in the rest frame is

$$\tau_{\text{GW}} \equiv f_p \frac{dt_p}{df_p}. \quad (2.7)$$

This timescale is given by

$$\tau_{\text{GW}}(M_1, M_2, f_p, e) = \frac{\tau_{\text{GW,circ}}(M_1, M_2, f_p)}{F(e)}, \quad (2.8)$$

where $\tau_{\text{GW,circ}}(M_1, M_2, f_p)$ is the timescale of GW emission by a binary in a circular orbit. This timescale is given by

$$\begin{aligned} \tau_{\text{GW,circ}}(M_1, M_2, f_p) &= \frac{5}{96} \left(\frac{c^3}{GM_{\text{chirp}}} \right)^{5/3} (2\pi f_p)^{-8/3} \\ &= 1.2 \times 10^4 \left(\frac{M_{\text{chirp}}}{10^8 M_{\odot}} \right)^{-5/3} \left(\frac{2f_p}{10^{-7} \text{ Hz}} \right)^{-8/3} \text{ yr}. \end{aligned} \quad (2.9)$$

As a result of the GW emission, the binary loses energy and angular momentum, and as a result, the orbit of the binary becomes more circular. The evolutions of the semi-major axis a and the eccentricity e are described by the follows,

$$\begin{aligned} \frac{da}{dt} &= -\frac{64}{5} \frac{G^3 M_1 M_2 M_{\text{tot}}}{c^5 a^3 (1 - e^2)^{7/2}} \left(1 + \frac{73}{24} e^2 + \frac{37}{96} e^4 \right) \\ &= -\frac{64}{5} \frac{G^3 M_1 M_2 M_{\text{tot}}}{c^5 a^3} F(e), \end{aligned} \quad (2.10)$$

$$\frac{de}{dt} = -\frac{304}{15} \frac{G^3 M_1 M_2 M_{\text{tot}}}{c^5 a^4 (1 - e^2)^{5/2}} e \left(1 + \frac{121}{304} e^2 \right), \quad (2.11)$$

where $M_{\text{tot}} \equiv M_1 + M_2$. Starting from a given orbit with parameters a_0 and e_0 , Eqs. (2.10) and (2.11) give the following relation between a and e :

$$\frac{a}{a_0} = \frac{1 - e_0^2}{1 - e^2} \left(\frac{e}{e_0} \right)^{\frac{12}{19}} \left[\frac{1 + \frac{121}{304} e^2}{1 + \frac{121}{304} e_0^2} \right]^{\frac{870}{2299}}. \quad (2.12)$$

From the equality $a^3 = GM_{\text{tot}}/(2\pi f_p)^2$, we find that the relation between the orbital frequency and the eccentricity is given by

$$\frac{f_p}{f_{p,0}} = \left\{ \frac{1 - e_0^2}{1 - e^2} \left(\frac{e}{e_0} \right)^{\frac{12}{19}} \left[\frac{1 + \frac{121}{304} e^2}{1 + \frac{121}{304} e_0^2} \right]^{\frac{870}{2299}} \right\}^{-3/2}, \quad (2.13)$$

where $f_{p,0}$ is the initial orbital frequency. In Fig. 1, we plot the evolution of the eccentricity as a function of the orbital frequency, $f_p/f_{p,0}$.

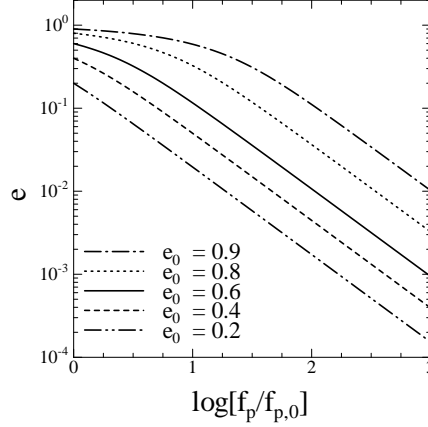


Fig. 1. Evolution of the eccentricity, $e = e(f_p/f_{p,0}, e_0)$, as a function of the orbital frequency, $f_p/f_{p,0}$, for $e_0 = 0.2, 0.4, 0.6, 0.8$ and 0.9 .

§3. GWBR from binaries in eccentric orbits

3.1. Characteristic amplitude of the GWBR spectrum

In any homogeneous and isotropic universe, the present-day GWBR energy density, $\rho_{\text{GW}}c^2$, must be equal to the sum of the energy densities radiated at each redshift z , divided by $(1+z)$ to account for the redshifting:

$$\rho_{\text{GW}}c^2 = \int_0^\infty \int_0^\infty n_c(z) \frac{1}{1+z} \frac{dE_{\text{GW}}}{df_r} df_r dz \quad (3.1)$$

$$= \int_0^\infty \int_0^\infty n_c(z) \frac{1}{1+z} f_r \frac{dE_{\text{GW}}}{df_r} dz \frac{df}{f}. \quad (3.2)$$

Here, $n_c(z)dz$ is the comoving number density of GW sources at redshifts in the range $z - z + dz$. Also f_r is the GW frequency in the source's *rest frame*, and f is the GW frequency in the *observer frame*, and thus we have $f_r = f(1+z)$. The quantity

$$\frac{dE_{\text{GW}}}{df_r} df_r \quad (3.3)$$

is the total energy emitted in GWs between the frequencies f_r and $f_r + df_r$. This energy is measured in the source's rest frame, and it is integrated over all solid angles and over the entire radiating lifetime of the source. Then, the total present-day energy density in GWs is

$$\rho_{\text{GW}}c^2 \equiv \int_0^\infty \frac{\pi c^2}{4G} f^2 h_c^2(\ln f) \frac{df}{f}, \quad (3.4)$$

where $h_c(\ln f)$ is the characteristic amplitude of the GWBR power spectrum over a logarithmic frequency interval $d \ln f = df/f$. Therefore, we find

$$\begin{aligned} h_c^2(\ln f) &= \frac{4G}{\pi c^2 f^2} \int_0^\infty n_c(z) \frac{1}{1+z} \left(f_r \frac{dE_{\text{GW}}}{df_r} \right) \Big|_{f_r=f(1+z)} dz, \\ &= \frac{4G}{\pi c^2 f} \int_0^\infty n_c(z) \left(\frac{dE_{\text{GW}}}{df_r} \right) \Big|_{f_r=f(1+z)} dz. \end{aligned} \quad (3.5)$$

If the GW sources are coalescing binaries, the characteristic amplitude is given by

$$h_c^2(\ln f) = \frac{4G}{\pi c^2 f} \int dM_1 dM_2 dz n_c(M_1, M_2, z) \left(\frac{dE_{\text{GW}}(M_1, M_2)}{df_r} \right) \Big|_{f_r=f(1+z)}. \quad (3.6)$$

where $n_c(M_1, M_2, z) dM_1 dM_2 dz$ is the comoving number density of coalescing binaries with masses $M_1 - M_1 + dM_1$ and $M_2 - M_2 + dM_2$ for $z - z + dz$.

Note that Eq. (3.5) assumes that the timescale of GW emission is much shorter than the Hubble time. This relationship between the power spectrum of the GWBR produced by cosmological GW sources and the SED of an individual source was derived by Phinney.¹⁴⁾

3.2. Total energy emitted in GWs

The total energy of GW radiation emitted over a lifetime of duration t_{life} is

$$E_{\text{GW}} = \int_0^{t_{\text{life}}} L_{\text{GW}}(t_p) dt_p \quad (3.7)$$

$$= \int_0^{t_{\text{life}}} \int L_{f_r}(t_p) df_r dt_p, \quad (3.8)$$

where $L_{\text{GW}}(t_p)$ is the power of GW emission and $L_{f_r}(t_p)$ is the SED of GW emission. Then, we have

$$\frac{dE_{\text{GW}}}{df_r} = \int_0^{t_{\text{life}}} L_{f_r}(t_p) dt_p. \quad (3.9)$$

Therefore, given the number density and SED of GW sources, we can calculate the amplitude of the GWBR power spectrum.

3.3. Characteristic amplitude of the GWBR spectrum from eccentric binaries

For a Keplerian binary consisting of two point masses M_1 and M_2 with an orbital eccentricity e , the SED of the GW radiation is given by Eq. (2.6). From Eqs. (2.6), (2.7) and (3.9), we obtain

$$\begin{aligned} \frac{dE_{\text{GW}}}{df_r} &= \int L_{\text{GW,circ}}(f_p) \frac{dt_p}{df_p} \sum_{n=1}^{\infty} g(n, e) \delta(f_r - n f_p) df_p \\ &= \sum_{n=1}^{\infty} \left[L_{\text{GW,circ}}(f_p) \frac{\tau_{\text{GW}}(f_p, e)}{n f_p} g(n, e) \right] \Big|_{f_p=f_r/n}. \end{aligned} \quad (3.10)$$

Thus, from Eqs. (3·6) and (3·10), the power spectrum of GWBR from binaries in eccentric orbits is given by

$$\begin{aligned} h_c^2(\ln f) &= \frac{4G}{\pi c^2 f} \int dM_1 dM_2 dz n_c(M_1, M_2, z) \sum_{n=1}^{\infty} \left[L_{\text{GW,circ}}(f_p) \frac{\tau_{\text{GW}}(f_p, e)}{n f_p} g(n, e) \right] \Big|_{f_p=f(1+z)/n} \\ &= \frac{4\pi c^3}{3} \int dM_1 dM_2 dz n_c(M_1, M_2, z) (1+z)^{-1/3} \left(\frac{GM_{\text{chirp}}}{c^3} \right)^{5/3} (\pi f)^{-4/3} \Phi, \end{aligned} \quad (3·11)$$

where

$$\Phi \equiv \sum_{n=1}^{\infty} \Phi_n \quad (3·12)$$

and

$$\Phi_n \equiv \left(\frac{2}{n} \right)^{2/3} \frac{g(n, e)}{F(e)}. \quad (3·13)$$

The left panel of Fig. 2 plots $g(n, e)$ as a function of the eccentricity, e , and the right panel plots Φ and Φ_n as functions of e .

Here we note that the eccentricity is a function of the orbital frequency, $f_p/f_{p,0}$, [see Eq. (2·13) and Fig. 1]. Therefore, $e = e(f_p/f_{p,0}, e_0) = e(f_r/nf_{p,0}, e_0) = e[f(1+z)/nf_{p,0}, e_0]$. Hence, Φ depends on f , $f_{p,0}$, e_0 and z . Since SMBH binaries have various initial eccentricities, the number density in Eq. (3·11) should be $n_c(M_1, M_2, e_0, z)$ and it should be integrated over e_0 . If all binaries are circular (i.e., $e_0 = 0$), $\Phi_2 = 1$ and $\Phi_n = 0$ for $n \neq 2$. Thus, we have $h_c \propto f^{-2/3}$ for $e_0 = 0$. By contrast, for $e_0 \neq 0$, Φ depends on f , and h_c is not proportional to $f^{-2/3}$. Therefore, Φ indicates the strength of the effect of orbital eccentricity on the GWBR power spectrum. In the left panel of Fig. 3, we plot Φ as a function of rest-frame GW frequency, $f_r/f_{p,0}$, for some initial eccentricities. In the right panel of Fig. 3, we plot Φ_n with $e_0 = 0.8$ as a function of $f_r/f_{p,0}$ for some harmonics. Owing to the radiation of the harmonics of f_p , the power spectrum is suppressed at lower frequencies, i.e. $f_r/f_{p,0} \lesssim 10$, and it is amplified at intermediate frequencies, i.e. $10 \lesssim f_r/f_{p,0} \lesssim 100$. For larger frequencies, $100 \lesssim f_r/f_{p,0}$, the main contributors to the power spectrum are circular binaries, which evolve from eccentric binaries and radiate only through the $n = 2$ mode.

§4. Power spectrum of the GWBR from eccentric SMBH binaries

4.1. A unified semi-analytic model of galaxy and SMBH formation

In order to predict the power spectrum of the GWBR from coalescing SMBH binaries, we must estimate the number density of coalescing SMBH binaries. To do this, we use a semi-analytic (SA) model¹⁷⁾ in which SMBH formation is incorporated into galaxy formation.¹⁶⁾

In the standard hierarchical structure formation scenario in a cold dark matter (CDM) universe, dark-matter halos (*dark halos*) cluster through the effect of gravity

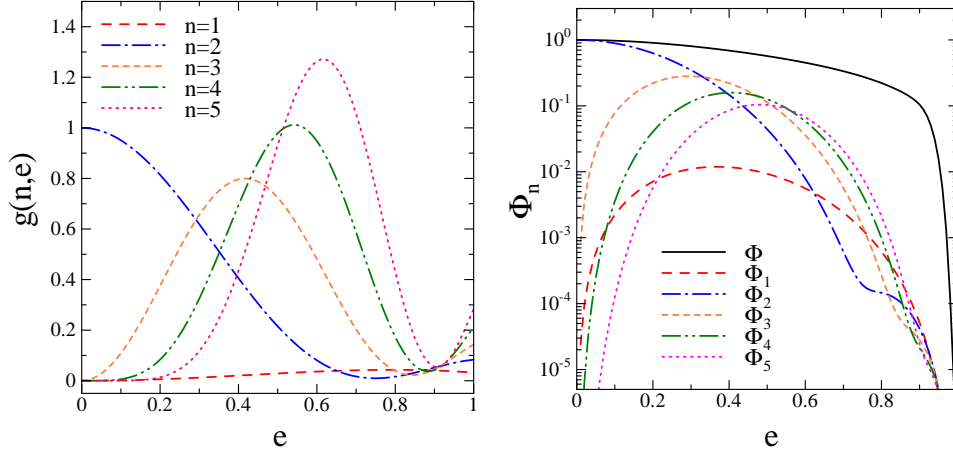


Fig. 2. Left panel: $g(n,e)$ as a function of e for $n = 1, 2, 3, 4$ and 5 . Right panel: Φ and Φ_n for $n = 1, 2, 3, 4$ and 5 as functions of e .

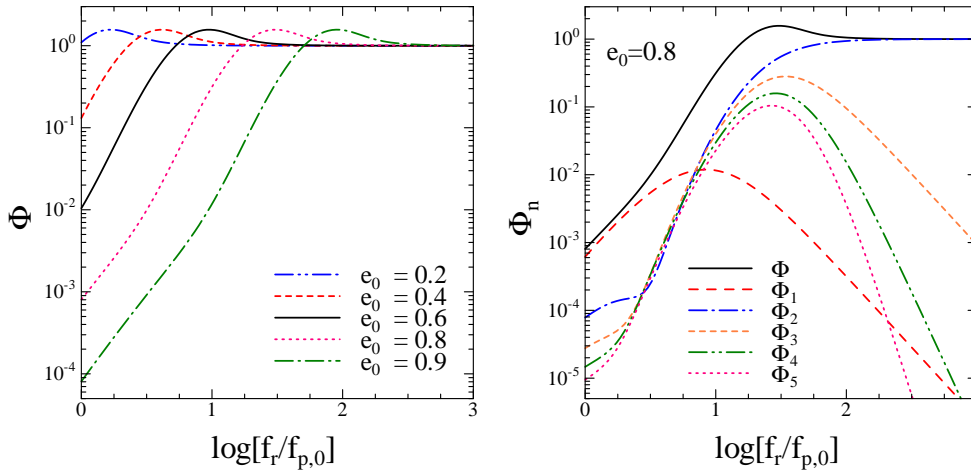


Fig. 3. Strength of the effect of the orbital eccentricity on the GWBR power spectra. Left panel: $\Phi = \Phi(f_r/f_{p,0}, e_0)$ as a function of $f_r/f_{p,0}$ for $e_0 = 0.2, 0.4, 0.6, 0.8$ and 0.9 . Right panel: Φ_n with $e_0 = 0.8$ as a function of $f_r/f_{p,0}$ for $n = 1, 2, 3, 4$ and 5 . Φ for $e_0 = 0.8$ is also shown.

and merge. In each merged dark halo, a galaxy is formed as a result of radiative gas cooling. In each galaxy, star formation and supernova feedback occur. Several galaxies in a common dark halo sometimes merge, and a more massive galaxy is thereby formed. When galaxies merge, SMBHs in the centers of these galaxies move toward the center of the new merged galaxy and subsequently form a SMBH binary. If the binary loses a sufficient amount of energy and angular momentum, it will evolve into the GW emitting regime and begin inspiraling, eventually coalescing with a GW burst.

In SA models, merging histories of dark halos are realized using a Monte-Carlo algorithm, and the evolution of baryonic components within dark halos is calculated

using simple analytic models for gas cooling, star formation, supernova feedback, galaxy merging and other processes. SA models have successfully reproduced a variety of observed features of galaxies, such as their luminosity functions and gas fractions in disk galaxies. In our SA model in which SMBH formation has been incorporated,¹⁷⁾ it is assumed that SMBHs grow through the coalescence of two or more SMBHs when their host galaxies merge. We also assume that during a major merger, a fraction of the cold gas proportional to the total mass of stars newly formed at the starburst is accreted onto the newly formed SMBH and that this gas fueling leads to quasar activity. Thus, SMBHs also grow through the accretion of cold gas. Our SA model reproduces not only observational features of galaxies¹⁶⁾ but also the present-day observed SMBH mass function and the quasar luminosity functions at different redshifts.¹⁷⁾ Using this SA model, Enoki et al. estimated the amplitude of GWBR from inspiraling SMBH binaries in circular orbits and the event rate of GW bursts due to SMBH binary coalescing.¹⁾

It is difficult to determine how SMBH binaries manage to shrink into a regime in which their evolution is driven by GW emission after their host galaxies merge, because not all the physical processes and conditions related to this problem (dynamical friction, the stellar distribution, triplet SMBH interaction, gas dynamical effects, and so on) are yet clear (see, e.g. Refs.^{7),8)} and¹⁸⁾). Therefore, it is also difficult to predict the distribution of the initial eccentricity. In what follows, for simplicity, we assume that all SMBH binaries coalesce when host galaxies merge. In other words, the efficiency of SMBH coalescence is assumed to be maximal. Thus, the efficiency of SMBH coalescence is maximal and the predicted amplitude of the GWBR spectrum should be interpreted as the upper limit (see Enoki et al.¹⁾). In this paper, in order to clarify the effect of eccentricity, we assume that all binaries have a single initial eccentricity given at a radius that is equal to some constant times the Schwarzschild radius of the SMBH.

In this study, the adopted cosmological model is a low-density, spatially flat cold dark matter (Λ CDM) universe with the present density parameter, $\Omega_m = 0.3$, the cosmological constant $\Omega_\Lambda = 0.7$, and the Hubble constant $h = 0.7$ ($h \equiv H_0/100 \text{ km s}^{-1} \text{ Mpc}^{-1}$). A detailed description of the model and its parameters is given in Nagashima et al.¹⁶⁾ and Enoki et al.^{1),17)}

4.2. Maximum orbital frequency

Substituting the number density of coalescing SMBH binaries, $n_c(M_1, M_2, z)dM_1dM_2dz$, into Eq. (3.11), we can calculate the power spectrum of the GWBR from SMBH coalescing SMBH binaries. Here, we introduce the cut off orbital frequency $f_{p,\text{max}}$.¹⁾ As a binary evolves with time owing to its emission of GW, the frequency increases. We assume that the binary orbit is quasi-stationary until the radius equals $3R_S$, where R_S is the Schwarzschild radius, i.e. the radius of the innermost stable circular orbit (ISCO) for a particle around a non-rotating black hole. Then, the maximum orbital frequency $f_{p,\text{max}}$ is

$$f_{p,\text{max}}(M_1, M_2) = \frac{c^3}{6^{3/2} 2\pi G M_1} \left(1 + \frac{M_2}{M_1}\right)^{1/2}$$

$$= 2.2 \times 10^{-5} \left(\frac{M_1}{10^8 M_\odot} \right)^{-1} \left(1 + \frac{M_2}{M_1} \right)^{1/2} \text{ Hz}, \quad (4.1)$$

where M_1 and M_2 are the SMBH masses (and we assume $M_1 > M_2$). Then, in Eq. (2.6), we replace $L_{\text{GW,circ}}(f_p)$ by $L_{\text{GW,circ}}(f_p)\theta(f_{p,\text{max}} - f_p)$, where $\theta(x)$ is the step function. Therefore, Φ_n becomes

$$\Phi_n = \left(\frac{2}{n} \right)^{2/3} \frac{g(n, e)}{F(e)} \theta(f_{p,\text{max}} - f(1+z)/n). \quad (4.2)$$

If this cut off does not exist, we have $h_c \propto f^{-2/3}$ for $f \gtrsim 2f_{p,\text{max}}$.

4.3. Results

In the left panel of Fig. 4, we plot power spectra of GWBR, h_c , from SMBH binaries for various initial eccentricities. The initial eccentricities, e_0 , are those at $f_{p,0}/f_{p,\text{max}} = 10^{-3}$ ($a = 300R_S$). This figure shows that power spectra at the frequencies measured by pulsar timing ($\sim 1 \text{ n} - 100 \text{ nHz}$) are suppressed as a result of harmonic radiation, especially for $e_0 \gtrsim 0.4$. The slope of the spectrum changes near $f = 1 \mu\text{Hz}$, owing to a lack of power associated with the upper limit frequency, $f_{p,\text{max}}$.

The right panel of Fig. 4 displays power spectra of GWBR from SMBH binaries for $e_0 = 0.8$ for different initial orbital frequencies with $f_{p,0}/f_{p,\text{max}} = 5^{-3}, 10^{-3}, 20^{-3}$ and 30^{-3} . Because $a \propto f_p^{-2/3}$, these correspond to $a = 75 R_S, 300 R_S, 1200 R_S$ and $2700 R_S$, respectively. Even in the case $f_{p,0}/f_{p,\text{max}} = 30^{-3}$, the power spectrum for $f \lesssim 1 \text{ nHz}$ is suppressed. We note that for a binary with $e_0 = 0.8$ at $f_{p,0}/f_{p,\text{max}} = 30^{-3}$ ($a = 2700R_S$), the eccentricity of the binary is $e \sim 0.95$ for $a \sim 10^4 R_S \sim 0.1 (M_{\text{BH}}/10^8 M_\odot) \text{ pc}$. Both panels of Fig. 4 indicate that the shape of the power spectrum in the low frequency range depends strongly on e_0 and $f_{p,0}/f_{p,\text{max}}$.

In Fig. 5, we plot some harmonics of the GWBR power spectrum from SMBH binaries for $e_0 = 0.8$ and $f_{p,0}/f_{p,\text{max}} = 10^{-3}$. As with the right panel of Fig. 3, in the lower frequency range, $f \lesssim 1 \text{ nHz}$, the $n = 1$ mode is dominant and in the higher frequency range, $f \gtrsim 0.1 \mu\text{Hz}$, the $n = 2$ mode is dominant. Therefore, in this frequency range, GWs from circular binaries are dominant.

The present-day energy density parameter of GWBR over a logarithmic frequency interval $d \ln f = df/f$ is given by

$$\Omega_{\text{GW}}(\ln f) = \frac{2\pi^2}{3H_0^2} f^2 h_c^2(\ln f). \quad (4.3)$$

In Fig. 6, we plot $\Omega_{\text{GW}}(\ln f)$ from SMBH binaries with $e_0 = 0.8$ and $f_{p,0}/f_{p,\text{max}} = 10^{-3}$ and with $e_0 = 0$ for several intervals of the total SMBHs mass ($M_{\text{tot}} = M_1 + M_2$). It is seen that the main contribution to the energy density is from binaries with total masses $M_{\text{tot}} = 10^7 - 10^{10} M_\odot$. In the lower frequency range ($f \lesssim 0.1 \mu\text{Hz}$), which can be measured by pulsar timing, GWs from binaries with masses $M_{\text{tot}} \geq 10^9 M_\odot$ are dominant. As with the left panel of Fig. 3, Fig. 6 shows suppressions and amplifications of the energy density parameters for each SMBH mass interval due to the

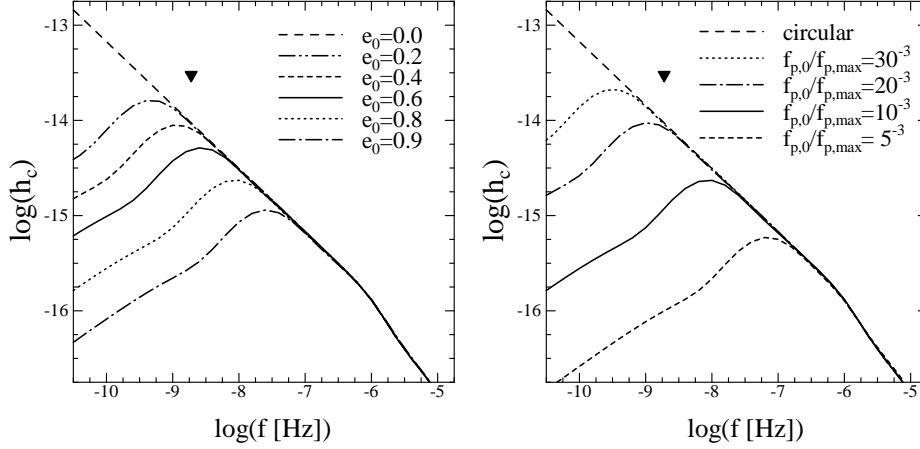


Fig. 4. Characteristic amplitudes of GWBR power spectra over a logarithmic frequency interval, $h_c(\ln f)$, from SMBH binaries. Left panel: Power spectra of GWBR from SMBH binaries with $f_{p,0}/f_{p,max} = 10^{-3}$ for several initial eccentricities, $e_0 = 0.0, 0.2, 0.4, 0.6, 0.8$ and 0.9 . Right panel: Power spectra of GWBR from SMBH binaries for $e_0 = 0.8$ for several initial orbital frequencies, $f_{p,0}/f_{p,max} = 5^{-3}, 10^{-3}, 20^{-3}$ and 30^{-3} . In each panel, the solid triangle indicates the current limit from pulsar timing measurements.¹⁹⁾

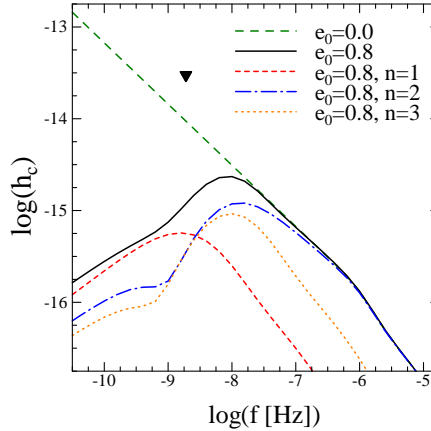


Fig. 5. Power spectra of GWBR from SMBH binaries for $e_0 = 0.8$. Some harmonics of the GWBR spectrum for $n = 1, 2$ and 3 . The initial orbital frequency is $f_{p,0}/f_{p,max} = 10^{-3}$. We also plot the power spectrum of GWBR from circular binaries (dashed line) and the current limit from pulsar timing measurements (solid triangle).¹⁹⁾

harmonic radiation. Here, the initial eccentricity is that at $f_{p,0}/f_{p,max} = 10^{-3}$. From Eq. (4-1), we find $f_{p,0} \propto f_{p,max} \propto (M_1 M_{tot})^{-1/2}$. Thus, for smaller-mass SMBHs, non-zero eccentricities affect the power of higher frequencies. When we sum up the energy densities of GWBR from SMBH mass intervals at approximately 10 nHz, where the energy density of GWBR from SMBH binaries with $M_{tot} > 10^9 M_\odot$ increases, the energy density of GWBR from SMBH binaries with $M_{tot} < 10^9 M_\odot$ has decreased significantly. For this reason, we cannot observe the amplification of the

total energy density of GWBR from SMBH binaries.

Pulsar timing measurements allow GWs with frequencies in the range 1 n – 100 nHz to be detected. Under the assumption that $h_c \propto f^{-2/3}$, the completed PPTA data set (twenty pulsars with an rms timing residual of 100 ns over 5 years) could potentially provide limits on the level of GWBR from SMBH binaries: $\Omega_{\text{GW}} = 5.5 \times 10^{-10}$ at $f = 10^{-7.5}$ Hz (1 yr⁻¹), $\Omega_{\text{GW}} = 1.3 \times 10^{-10}$ at $f = 10^{-8.4}$ Hz (1/8 yr⁻¹) and $\Omega_{\text{GW}} = 7.3 \times 10^{-11}$ at $f = 10^{-8.8}$ Hz (1/20 yr⁻¹).²⁰⁾ In Fig. 6, we also plot the potential future limits. These limits are well under the predicted energy density of GWBR from SMBH binaries for $e_0 = 0$ ($h_c \propto f^{-2/3}$). Therefore, we conclude that the full PPTA data set should be sufficient to constrain the effect of eccentricity on the GWBR from SMBH binaries.

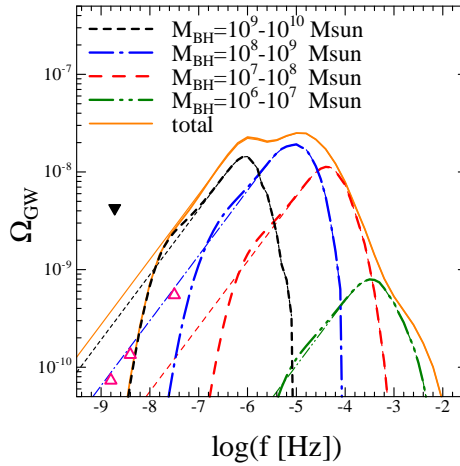


Fig. 6. Energy density parameters of GWBR over a logarithmic frequency interval $\Omega_{\text{GW}}(\ln f)$ in several intervals of the total mass. The thick curves represent the results for $e_0 = 0.8$ and $f_{p,0}/f_{p,\text{max}} = 10^{-3}$, and thin curves represent the results for $e_0 = 0$. The solid triangle indicates the current limit from pulsar timing measurements.¹⁹⁾ The three other triangles indicate the potential future lower limits from the full PPTA data set for the case $h_c \propto f^{-2/3}$.²⁰⁾

4.4. Effects of galaxy formation processes on GWBR from SMBH binaries

The number density of coalescing SMBH binaries with masses in the range $M_1 - M_1 + dM_1$ and $M_2 - M_2 + dM_2$ at $z - z + dz$, i.e. $n_c(M_1, M_2, z)dM_1dM_2dz$, depends on galaxy formation processes. In our SA model, the dominant mass growth process of SMBHs is the accretion of cold gas, which is also the material of stars.¹⁾ Thus, $n_c(M_1, M_2, z)$ depends strongly on processes related to star formation related. Here, we show how the star formation time scale and the strength of supernova feedback affect the power spectrum of the GWBR from SMBH binaries.

In our SA model, the star formation rate (SFR) of a galaxy is assumed to be $\dot{M}_* = M_{\text{cold}}/\tau_*$, where M_{cold} is the mass of the cold gas and τ_* is the time scale of star formation. We assume $\tau_* = \tau_*^0 (V_{\text{circ}}/300 \text{ km s}^{-1})^{\alpha_*}$, where V_{circ} is the circular velocity of the galaxy. The free parameters τ_*^0 and α_* are chosen to match the observed mass fraction of cold gas in the disks of spiral galaxies. With

star formation, supernovae occur and heat up the surrounding cold gas, yielding a hot gas phase (a process called supernova feedback). The reheating rate is given by $\dot{M}_{\text{reheat}} = \beta(V_{\text{circ}})\dot{M}_*$, where $\beta(V_{\text{circ}}) = (V_{\text{hot}}/V_{\text{circ}})^{\alpha_{\text{hot}}}$. The free parameters V_{hot} and α_{hot} are determined by matching the observed local luminosity function of galaxies. In a previous study¹⁾ (and in a previous subsection of this paper), we adopted $\tau_*^0 = 1.5$ Gyr, $\alpha_* = -2$, $V_{\text{hot}} = 280$ km s⁻¹ and $\alpha_{\text{hot}} = 2.5$ as fiducial values.

The left panel of Fig. 7 displays power spectra of GWBR from SMBH binaries for various star formation time scales, τ_*^0 . Other parameters are the same in each case. It is seen that for large τ_*^0 , the SFR is small and thus a large amount of cold gas remains in each galaxy. Thus, the masses of SMBHs become large. Therefore, the amplitude of the power spectrum of the GWBR becomes large. Moreover, the slope changing frequency moves forward lower frequency, because the upper limit frequency, $f_{p,\text{max}}$, becomes small. The right panel of Fig. 7 plots power spectra of GWBR from SMBH binaries for various supernovae feedback strengths, V_{hot} . Other parameters are the same in each case. In the case of no supernovae feedback ($V_{\text{hot}} = 0$ km s⁻¹), the cold gas is not heated to a hot gas. Thus, a large amount of cold gas remains in each galaxy, and the masses of SMBHs become large. By contrast, for the large V_{hot} case, the cold gas is greatly heated, and thus the masses of SMBH become small. Both panels of Fig. 7 indicate that although the shape of the power spectrum of the GWBR from SMBH binaries is affected by the eccentricity of binaries for low frequencies, $f \lesssim 1$ nHz, the shape of the power spectrum for higher frequencies and the overall amplitude depend strongly on the processes of galaxy formation.

We note that the purpose of this subsection is to demonstrate the importance of galaxy formation processes on the growth of SMBHs and the GWBR from SMBH binaries. Therefore, in this subsection, we present cases with *extreme parameter values*. Results for models with these parameter values are greatly inconsistent with observational results, such as galaxy luminosity functions and the present SMBH mass function. In Fig. 8, we plot SMBH mass functions at $z = 0$. It is seen that only the model with fiducial values is consistent with the observational results obtained by Salucci et al.²¹⁾

§5. Summary and conclusions

In this study, we have investigated how orbital eccentricities of binaries affect power spectra of GWBR from coalescing SMBH binaries. A compact binary in an eccentric orbit radiates GWs at all integer harmonics of its orbital frequency. Owing to this harmonic radiation, the SED, the power and the timescale of the GW emission of a binary in an eccentric orbit are different from those of a binary in a circular orbit. Therefore, first, we formulated the power spectrum of GWBR from cosmological compact binaries in eccentric orbits. Then using this formulation and our SA model for galaxy and SMBH formation, we calculated the power spectra of GWBR from coalescing SMBH binaries in eccentric orbits.

We found that the calculated power spectra of the GWBR from SMBH binaries in eccentric orbits are suppressed owing to the harmonic radiation for lower frequencies ($f \lesssim 1$ nHz) if the initial eccentricity satisfies $e_0 > 0.2$ at $a = 300 R_S$. The

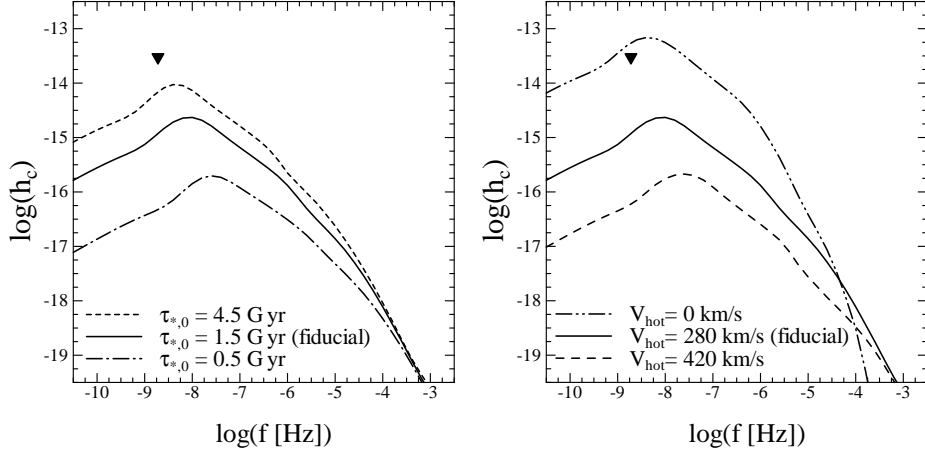


Fig. 7. Effects of galaxy formation processes on the power spectrum of GWBR from SMBH binaries with $e_0 = 0.8$ and $f_{p,0}/f_{p,\max} = 10^{-3}$. Left panel: For three star formation time scales, $\tau_{*,0} = 0.5, 1.5$ and 4.5 Gyr. Here $\tau_{*,0} = 1.5$ Gyr is the fiducial value. Right panel: For three supernovae feedback strengths, $V_{\text{hot}} = 0, 280$ and 420 km s $^{-1}$. Here, $V_{\text{hot}} = 280$ km s $^{-1}$ is the fiducial value. The case $V_{\text{hot}} = 0$ km s $^{-1}$ corresponds to no supernova feedback. In each panel, we also plot the current limit obtained from pulsar timing measurements (solid triangle).¹⁹⁾

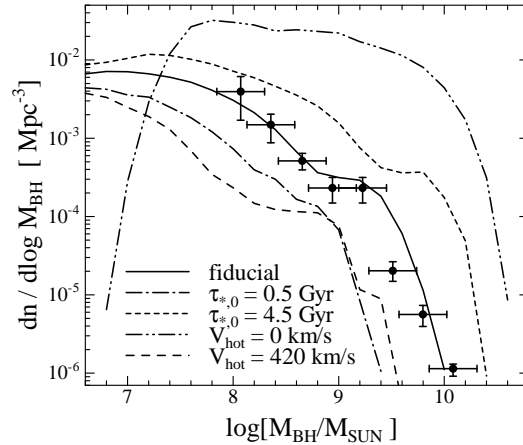


Fig. 8. SMBH mass functions of several models at $z = 0$. The solid curve represents the results of the model with fiducial values, $\tau_{*,0} = 1.5$ Gyr and $V_{\text{hot}} = 280$ km s $^{-1}$. The dots with error bars present the data for the present mass function obtained by Salucci et al.²¹⁾

degree of this suppression depends strongly on the initial eccentricity. In this paper, for simplicity and in order to clarify the effect of the eccentricity, we assumed that all binaries have the same initial eccentricity. The results of our study suggest that elucidating the initial eccentricity distribution is essential for the investigation of the power spectrum of GWBR from compact binaries.

Because the number density of coalescing SMBH binaries is determined by the processes of galaxy formation, the power spectrum of the GWBR from SMBH binaries depends strongly on these processes, especially processes related to star forma-

tion, which regulate the amount of cold gas accreted onto SMBHs. The prediction of our model shows that the overall shape and amplitude of the power spectrum of the GWBR from coalescing SMBH binaries depend on galaxy formation processes. However, for low frequencies ($f \lesssim 1$ nHz), the shape of the power spectrum of the GWBR also depends on the initial eccentricity. Because the pulsar timing measurements can provide limits on the level of GWBR with frequencies $f \sim 1$ n – 100 nHz, pulsar timing observations, such as PPTA project, should provide constraints not only on the number density of coalescing SMBH binaries but also on the effect of orbital eccentricity on the GWBR from SMBH binaries.

Acknowledgements

We thank Dr. K. T. Inoue for useful suggestions. The numerical computations in this work were partly carried out at the Astronomy Data Center of the National Astronomical Observatory of Japan. This work was supported in part by a Nagasaki University President’s Fund Grant.

References

- 1) M. Enoki, K. T. Inoue, M. Nagashima and N. Sugiyama, *Astrophys. J.* **615** (2004), 19.
- 2) M. Rajagopal and R. Romani, *Astrophys. J.* **446** (1995), 543.
A. H. Jaffe and D. C. Backer, *Astrophys. J.* **583** (2003), 616.
J. S. B. Wyithe and A. Loeb, *Astrophys. J.* **590** (2003), 691.
A. Sesana, F. Haardt, P. Madau and M. Volonteri, *Astrophys. J.* **611** (2004), 623.
- 3) A. J. Farmer and E. S. Phinney, *Mon. Not. R. Astron. Soc.* **346** (2003), 1197.
- 4) M. V. Sazhin, *Sov. Astron.* **22** (1978), 36.
S. Detweiler, *Astrophys. J.* **234** (1979), 1100.
- 5) F. A. Jenet, G. B. Hobbs, K. J. Lee and R. N. Manchester, *Astrophys. J.* **625** (2005), L123.
- 6) G. Hobbs, *Publ. Astron. Soc. Australia* **22** (2005), 179.
- 7) S. Mikkola and M. J. Valtonen, *Mon. Not. R. Astron. Soc.* **259** (1992), 115.
- 8) T. Fukushige, T. Ebisuzaki and J. Makino, *Publ. Astron. Soc. Jpn.* **44** (1992), 281.
- 9) M. Iwasawa, Y. Funato and J. Makino, *Astrophys. J.* **651** (2006), 1059.
- 10) T. Matsubayashi, J. Makino and T. Ebisuzaki, *Astrophys. J.* **656** (2007), 879.
- 11) P. J. Armitage and P. Natarajan, *Astrophys. J.* **634** (2005), 921.
- 12) P. C. Peters and J. Mathews, *Phys. Rev.* **131** (1963), 435.
P. C. Peters, *Phys. Rev.* **136** (1964), 1224.
- 13) M. Fitchett, *Mon. Not. R. Astron. Soc.* **224** (1987), 567.
- 14) E. S. Phinney, astro-ph/0108028.
- 15) K. Ioka, T. Tanaka and T. Nakamura, *Phys. Rev. D* **60** (1999), 083512.
V. B. Ignatiev, A. G. Kuranov, K. A. Postnov and M. E. Prokhorov, *Mon. Not. R. Astron. Soc.* **327** (2001), 531.
- 16) M. Nagashima, T. Totani, N. Gouda and Y. Yoshii, *Astrophys. J.* **557** (2001), 505.
M. Nagashima, Y. Yoshii, T. Totani and N. Gouda *Astrophys. J.* **578** (2002), 675.
- 17) M. Enoki, M. Nagashima and N. Gouda, *Publ. Astron. Soc. Jpn.* **55** (2003), 133.
- 18) M. C. Begelman, R. D. Blandford and M. J. Rees, *Nature* **287** (1980), 307.
J. Makino, *Astrophys. J.* **478** (1997), 58.
A. Gould and H. Rix, *Astrophys. J.* **532** (2000), L29.
Q. Yu, *Mon. Not. R. Astron. Soc.* **331** (2002), 935.
P. J. Armitage and P. Natarajan, *Astrophys. J.* **567** (2002), L9.
O. Blaes, M. H. Lee and A. Socrates, *Astrophys. J.* **578** (2002), 775.
M. Milosavljevic and D. Merritt, *Astrophys. J.* **596** (2003), 860.
J. Makino and Y. Funato, *Astrophys. J.* **602** (2004), 93.
C. Zire, *Mon. Not. R. Astron. Soc.* **371** (2006), L36; astro-ph/0610457.

- 19) A. N. Lommen, in *MPE Rep. 278, WE-Heraeus Seminar on Neutron Stars, Pulsars and Supernova Remnants*, ed. W. Becker, H. Lesch and J. Truemper (Garching, MPE, 2002).
- 20) F. A. Jenet et al., *Astrophys. J.* **653** (2006), 1571.
- 21) P. Salucci, E. Szuszkiewicz, P. Monaco and L. Danese, *Mon. Not. R. Astron. Soc.* **307** (1999), 637.